NANOSYSTEMS:
PHYSICS, CHEMISTRY, MATHEMATICS

Zirnik G.M., et al. *Nanosystems: Phys. Chem. Math.*, 2024, **15** (4), 520–529.
http://nanojournal.ifmo.ru
DOI 10.17586/2220-8054-2024-15-4-520-529

Original article

Phase formation of nanosized $InGaZnO_4$ obtained by the sol-gel method with different chelating agents

Gleb M. Zirnik[1,2], Alexander S. Chernukha[1,2,3], Daniil A. Uchaev[3], Ibrohimi A. Solizoda[1,2,4], Svetlana A. Gudkova[1,2], Nadezhda S. Nekorysnova[1], Denis A. Vinnik[1,2,3]

[1]Moscow Institute of Physics and Technology, Dolgoprudny, Russia

[2]St. Petersburg State University, St. Petersburg, Russia

[3]South Ural State University, Chelyabinsk, Russia

[4]Tajik National University, Dushanbe, Tajikistan

Corresponding author: Denis A. Vinnik, vinnikda@susu.ru

ABSTRACT The production of nano-sized semiconductor oxide materials, such as indium-gallium-zinc oxide (IGZO), will make it possible to use it for the transistors manufacture using printing methods. The sol-gel method is one of the widely known and used methods for producing nano-sized oxide materials. As is known, a chelating reagent (complexing agent) can influence both the synthesis process and the final phase composition. The results of sol-gel synthesis with various chelating reagents: citric acid, ethylene glycol, oxalic acid, urea, glycerol and sucrose are presented. The samples were studied by X-ray diffraction. It was found that ethylene glycol and glycerol as chelating reagents make it possible to obtain a homogeneous crystalline material at 900 °C with a $YbFe_2O_4$-type structure, R-3m (166) space group. Unit cell parameters and crystallite size (Halder-Wagner method) for $InGaZnO_4$ single-phase samples were calculated.

KEYWORDS indium-gallium-zinc oxide, In-Ga-Zn-O, IGZO, sol-gel method, complexing agent, chelating reagent, phase formation, nanomaterial

ACKNOWLEDGEMENTS This study represents an integration of two diverse projects supported by the Russian Science Foundation (No. 24-19-00468; conceptualization, comparative analysis of the chelating agents influence on the synthesis processes, as well as the synthesis and detailed characterization of samples IGZO-3, IGZO-4, IGZO-5, IGZO-6) and the Ministry of Science and Higher Education of the Russian Federation (Goszadaniye No. 075-03-2024-117, project No. FSMG-2024-0028; syntheses of IGZO-1 and IGZO-2 and its characterization).

FOR CITATION Zirnik G.M., Chernukha A.S., Uchaev D.A., Solizoda I.A., Gudkova S.A., Nekorysnova N.S., Vinnik D.A. Phase formation of nanosized $InGaZnO_4$ obtained by the sol-gel method with different chelating agents. *Nanosystems: Phys. Chem. Math.*, 2024, **15** (4), 520–529.

1. Introduction

Sol-gel technology makes it possible to obtain micro- and nanoparticles, including $InGaZnO_4$ material. Nanosized indium-gallium-zinc oxide (IGZO) production is extremely important, since it opens up the possibility of its use as an ink material for transistors printing [1–5].

Sol-gel technology is widely known. The most widely used technology, called the “Pechini method” or the “citrate gel” method, was patented by Maggio Pechini in 1967 [6]. Pechini proposed a method for titanates, zirconates, niobates of lead and alkaline earth metals obtaining. The method used a chelate reagent solution (citric acid in ethylene glycol) and the required oxide of metal, by evaporating the solvent, a transparent “gel” (the “resin” in original) was obtained, which was then heated to temperatures of 575 – 730 °C to obtain the final product. This synthesis method began to be successfully used to obtain other oxide materials later [7].

The literature contains a significant number of terms that essentially describe the same process, for example, “sol-gel method” [8], “sol-gel auto-combustion method” [9], “solution combustion synthesis” [10], “self-propagation combustion method” [11], “...mediated sol-gel combustion method” [12] (there is no common terminology). These terms often describe the same process in which desired metal nitrates react with organic complexing agents (which are also organic “fuels”) in an aqueous solution, after which a gel is formed. After this, the resulting material is slowly heated to the auto-combustion stage, during which nitrates act as the organic components oxidizers. The material obtained as an auto-combustion stage result described as a xerogel in the literature. The xerogel is ground and heated to remove the formed carbon to obtain the final material (with the required crystallinity).

When producing oxide materials by the sol-gel method, one chelating reagent is often used; two or more reagents are used less often. Also, the choice of a specific chelating reagent always remains unfounded. However, works that present

the study of several chelating reagents under the conditions of "sol-gel" synthesis have been found [13–15], but these studies are scarce and we have not found the preparation of IGZO with various chelating reagents in the sol-gel process in the literature.

The purpose of this work is to search for suitable complexing agents to obtain homogeneous $InGaZnO_4$ samples at a minimum temperature (to obtain IGZO nanoparticles).

2. Methodology of experimental research

The synthesis of $InGaZnO_4$ by sol-gel method was carried out according to the method below. Indium(III) nitrate 4.5-hydrate $In(NO_3)_3 \cdot 4.5H_2O$, gallium(III) nitrate nonahydrate $Ga(NO_3)_3 \cdot 9H_2O$, zinc(II) nitrate hexahydrate $Zn(NO_3)_2 \cdot 6H_2O$, citric acid, ethylene glycol, glycerol, urea, sucrose and oxalic acid was used for synthesis. All components were chemically pure. All metal nitrates used in the synthesis were preliminarily gravimetrically calcined at 800 °C for 12 hours. A correction was introduced into the nitrate samples according to gravimetric data. Reagents were weighed on a Scientech SA 80 analytical balance with an accuracy of 0.1 mg. Stirring, heating, and evaporation of solutions were carried out on a magnetic stirrer with heating Stegler HS Pro-DT. Further heating of the samples was carried out in a Nabertherm L9/12/P330 muffle furnace with a programmable temperature controller.

The masses of metal nitrates were calculated to achieve a molar ratio of In^{3+}:Ga^{3+}:Zn^{2+} = 1:1:1 in the product (the error in taking a sample of nitrates in all cases was no more than ± 0.001 g). The mass of salts was calculated to obtain 2.00 g of $InGaZnO_4$. The molar ratio of metal ions to complexing agent was chosen as Me^{x+}/ complexing agent = 1:3. Weighed amounts of salts and complexing agent were separately dissolved in distilled water with stirring. After this, an aqueous solution of a complexing agent was added to the aqueous solution of nitrates and it was evaporated with intense stirring to a viscous gel. Next, the material was placed in a muffle furnace and subjected to heat treatment to remove residual water and initiate an auto-combudtion reaction according to the following heating program: (i) heating up to 100 °C for 1 hour and holding at this temperature for 2 hours; (ii) heating up to 150 °C for 1 hour and holding at this temperature for 2 hours, (iii) heating up to 200 °C for 1 hour and holding at this temperature for 2 hours, (iv) cooling the samples in air and grinding to the powder, (v) heating up to 500 °C for 90 minutes and holding at this temperature for 6 hours, (vi) cooling samples in air, if necessary, taking part of the sample obtained at 500 °C for 6 hours and sintering at 700, 900 or 1000 °C for 12 hours, cooling the samples in air. Each of the syntheses was assigned a corresponding code: IGZO-1 for citric acid, IGZO-2 for ethylene glycol, IGZO-3 for oxalic acid, IGZO-4 for urea, IGZO-5 for glycerol and IGZO-6 for sucrose.

X-Ray diffraction (XRD) studies were carried out on a Rigaku Ultima IV powder X-ray diffractometer (CuKα, 40 kV, 30 mA; $\lambda = 0.15406$ nm, energy-dispersive semiconductor detector Rigaku D/teX Ultra) at a recording speed of 5 °/min. Before studies, the samples were ground in an agate mortar to the fine powder. Qualitative analysis was carried out using the STOE Win XPow software package. Lattice parameters refinement and crystallite size determination was carried out in the Rigaku PDXL software package by WPPF (whole-powder-pattern fitting) method. To refine the unit cell parameters of IGZO single-phase samples, diffraction patterns were recorded at 2 °/min speed. The crystal structure of $InGaZnO_4$ was visualized using the VESTA software package [16]. Scanning electron microscopy (SEM) was carried out on a Jeol JSM 7001F scanning electron microscope (accelerating voltage = 20 kV, a conductive gold layer was deposited on the substrate by magnetron sputtering). Transmission electron microscopy (TEM) was carried out on a high-resolution transmission microscope JEOL JEM-2600 at a 160 kV accelerating voltage.

3. Results and discussion

Structurally, $InGaZnO_4$ corresponds to the $YbFe_2O_4$ compound of the rhombohedral system with R-3m (166) space group [17]. The prototype contains di- and trivalent iron, which is conveniently represented by the formula $Yb^{3+}Fe^{3+}Fe^{2+}O_4$. In $InGaZnO_4$ structure, indium occupies ytterbium sites, gallium occupies Fe^{3+} sites, and zinc occupies Fe^{2+} sites [18]. In the structure of $InGaZnO_4$, layers can be distinguished. In a separate layer, indium atoms are located in a distorted InO_6 octahedron, and zinc and gallium atoms are in a separate layer in the center of the MO_5 trigonal bipyramid, where M is Zn or Ga (Fig. 1). Note that the distribution of gallium and zinc in one layer is not distinguishable by X-ray diffraction; for this reason, it is shown in Fig. 1 in the structural model, the positions of gallium and zinc were assumed to be equally probable. The diffraction pattern calculated for $InGaZnO_4$ based on literature data [19] is in good agreement with experiment (Fig. 2).

Diffraction patterns of the obtained $InGaZnO_4$ samples are presented in Figs. 3 – 8. It can be seen that in all cases, except for the IGZO-3 sample, the reflections of the main phase correspond to $InGaZnO_4$ [17]. The obtained diffraction patterns were analyzed for the presence of possible impurity phases in the material, such as In_2O_3 with a bixbyite structure [20], Ga_2O_3 of various modifications, ZnO, as well as binary compounds (In–Ga–O, In–Zn–O, Zn–Ga–O, for example $ZnGa_2O_4$ [21]) and ternary (In–Ga–Zn–O) oxide systems.

The numbers in brackets correspond to the Miller indices of the corresponding plane on the Fig. 7. It should be noted that for most samples there is an overlap of the most intense reflections of $InGaZnO_4$ and In_2O_3. Thus, for $InGaZnO_4$ and In_2O_3, the main reflections have Miller indices of 009 and 104, located in the diffraction pattern at 30.8 and 31.0 °2θ,

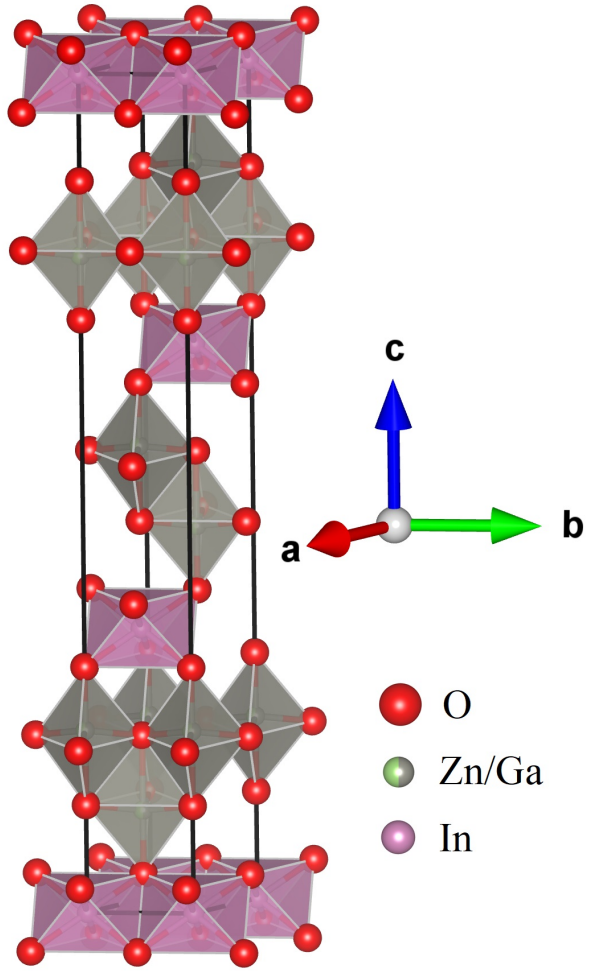

FIG. 1. Structural model of the unit cell of $InGaZnO_4$ consisting of InO_6 octahedra and MO_5 trigonal bipyramids, where M is Zn or Ga

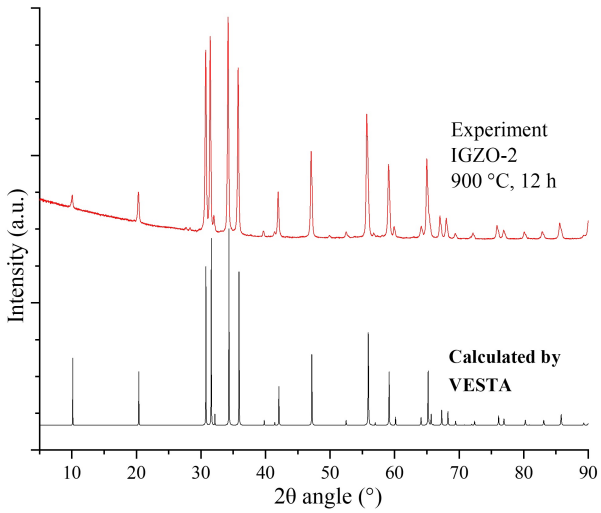

FIG. 2. Comparison of experimental and calculated diffraction patterns of $InGaZnO_4$. The calculation was performed in the VESTA software package based on data [19]

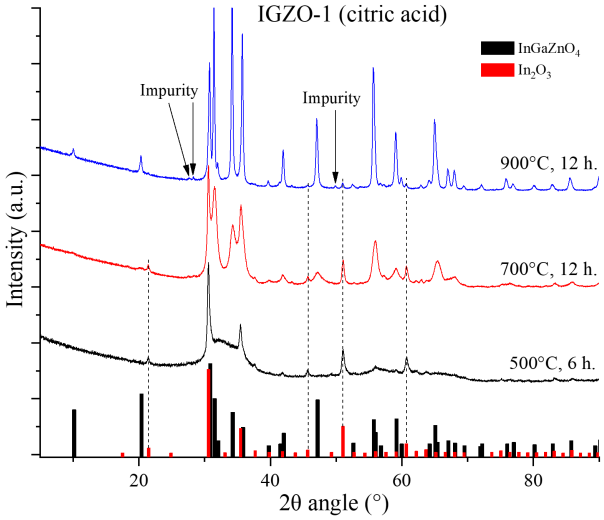

FIG. 3. XRD pattern of IGZO-1 prepared at 500, 700 and 900 °C. Black lines – $InGaZnO_4$ [17], red line – In_2O_3 [20]

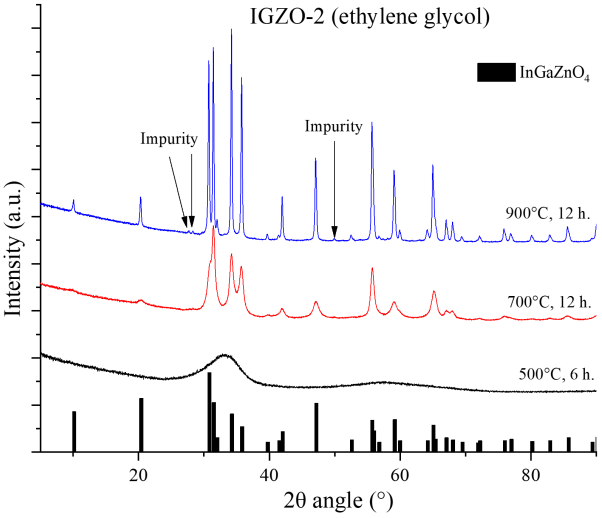

FIG. 4. XRD pattern of IGZO-2 prepared at 500, 700 and 900 °C. Black lines – $InGaZnO_4$ [17]

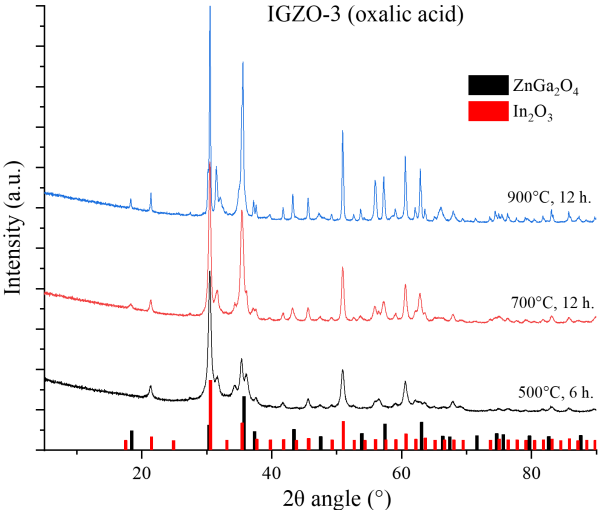

FIG. 5. XRD pattern of IGZO-3 prepared at 500, 700 and 900 °C. Black lines – $ZnGa_2O_4$ [21], red lines – In_2O_3 [20]

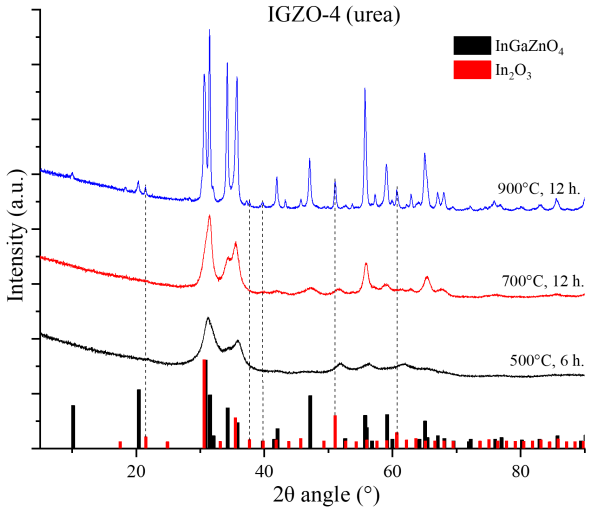

FIG. 6. XRD pattern of IGZO-4 prepared at 500, 700 and 900 °C. Black lines – $InGaZnO_4$ [17], red line – In_2O_3 [20]

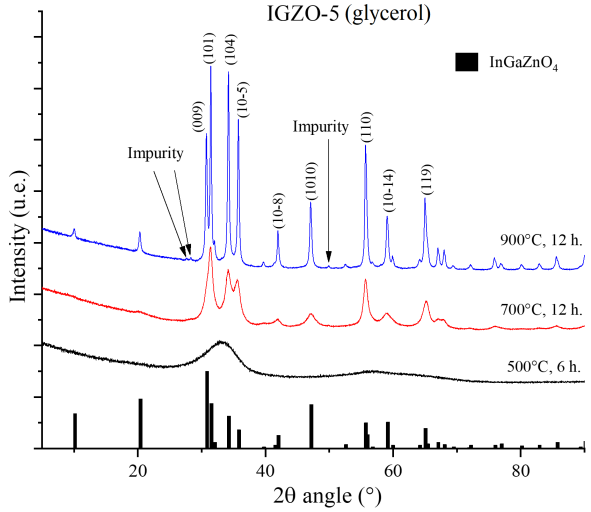

FIG. 7. XRD pattern of the IGZO-5 sample obtained at temperatures of 500, 700 and 900 °C. Black lines – $InGaZnO_4$ [17]

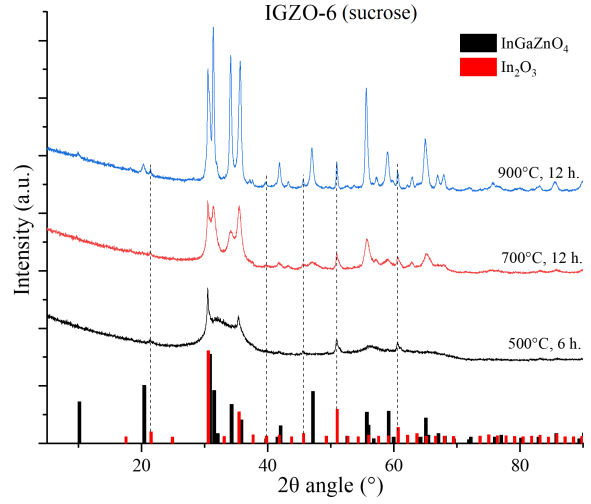

FIG. 8. XRD pattern of the IGZO-6, prepared at 500, 700 and 900 °C. Black lines – $InGaZnO_4$ [17], red lines – In_2O_3 [20]

respectively. Therefore, to detect In_2O_3 impurities in the composition of samples, use a less intense reflection, recorded at about 51.0 °2θ and corresponding to reflection from the (440) plane.

First consider the XRD results of non-single-phase samples. XRD patterns of IGZO-4 and IGZO-6 follow that they are a mixture of $InGaZnO_4$ and In_2O_3. Note that reflections corresponding to In_2O_3 appear in the IGZO-4 sample obtained at 500 °C, while the IGZO-6 sample at this temperature is still amorphous and does not contain crystalline phases. An increase in the sintering temperature causes an increase in the crystallinity of both the $InGaZnO_4$ and In_2O_3 phases. This can be seen from the decrease in the width of the reflections of these phases. In this case, the formation of a single-phase sample does not occur even at a temperature of 900 °C.

IGZO-3 at 500 °C is also non-single-phase sample. The main phases are solid solutions based on In_2O_3 [20] and $ZnGa_2O_4$ [21]. When the sintering temperature increases to 900 °C, reflections corresponding to the $InGaZnO_4$ phase appear, but its amount in the composition of this sample is minimal. Apparently, when using oxalic acid, individual metal oxalates are formed, for example: $Zn(C_2O_4)$, $Ga_2(C_2O_4)_3$ and $In_2(C_2O_4)_3$. Thus, when a solution of oxalic acid was introduced into a solution of metal nitrates, a white precipitate immediately formed, while other solutions remained transparent.

Samples IGZO-1, IGZO-2 and IGZO-5 are closest to the single-phase state. IGZO-1 sample obtained at 500 °C is a mixture of an amorphous material with crystalline indium oxide In_2O_3 (Fig. 3). However, as the temperature increases, the intensity of the In_2O_3 reflections decreases and for the sample obtained at 900 °C, their intensity becomes extremely low.

The IGZO-2 sample obtained with ethylene glycol at 500 °C is amorphous; at 700 °C – slightly crystallized. At these temperatures, no foreign phases were detected, however, the sample obtained at 900 °C contains foreign reflections at 27.7, 28.3 and 49.9 °2θ, which could not be identified (Fig. 4). The same reflections appear in the diffraction patterns of IGZO-1 and IGZO-5 obtained at 900 °C.

In order to achieve homogenization at higher temperatures, samples IGZO-1, IGZO-2 and IGZO-5 were additionally kept at a temperature of 1000 °C for 12 hours. The XRD pattern of samples are presented in Figs. 9 – 11.

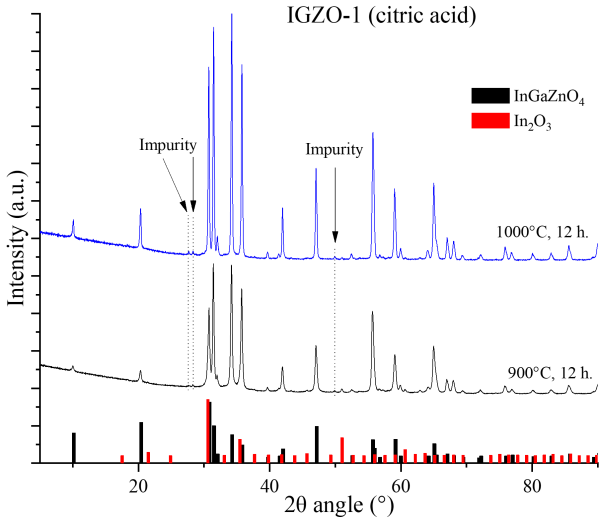

FIG. 9. XRD pattern of IGZO-1 prepared at 1000 °C. Black lines – $InGaZnO_4$ [17], red line – In_2O_3 [20]

As can be seen from the obtained XRD pattern (Figs. 9 – 11), for all samples, with increasing processing temperature, their crystallinity increases. Thus, the half-width of the reflection of the main phase of the IGZO-2 sample, located at about 34.2 °2θ, decreases when heated from 700 to 900 and 1000 °C, respectively, from 0.63 to 0.21 and further to 0.17 °2θ. For IGZO-1 and IGZO-5 samples, the decrease in the half-width of the reflection around 34.2 °2θ occurs in a similar way. Calcination at higher temperatures is not advisable, since this will cause growth and sintering of particles [22, 23], which will negatively affect the possibility of using this oxide material for the further production of nanopowders.

For IGZO-2 and IGZO-5 samples obtained at 700 and 900 °C and containing the least amount of impurities, the cell parameters and crystallite size were calculated (Tables 1 and 2). For the $InGaZnO_4$ material obtained at 1450 °C for 24 hours [17], the cell parameters are slightly smaller ($a = 3.295$ Å, $c = 26.07$ Å) than at 700 and 900 °C, but in general they coincide well with them. The crystallite size was calculated using the Halder-Wagner method [24] using the six most intense reflections (Fig. 12).

Figure 13 shows SEM and TEM micrographs of the IGZO-5 sample obtained at 500 °C for 6 hours. Both photographs clearly show that the material is an agglomerate of nanoparticles. SEM microphotography suggests that the size of most particles present in the cluster is less than 100 nm, but their exact size is difficult to determine. As can be seen from the TEM micrograph, the material actually consists of a large accumulation of particles, most of which have a size of about

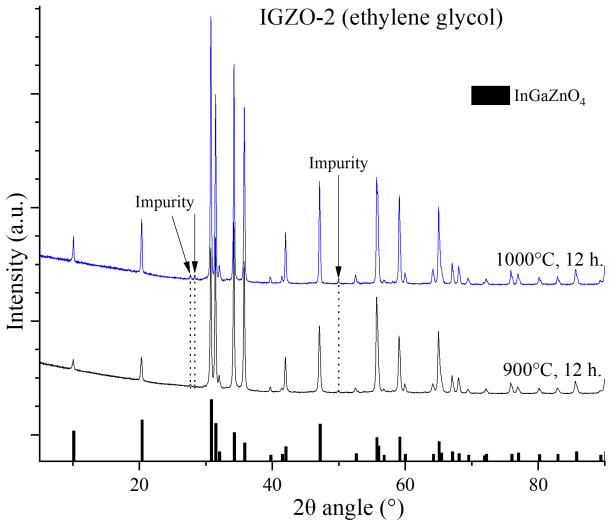

FIG. 10. XRD pattern of IGZO-2 prepared at 1000 °C. Black lines – $InGaZnO_4$ [17]

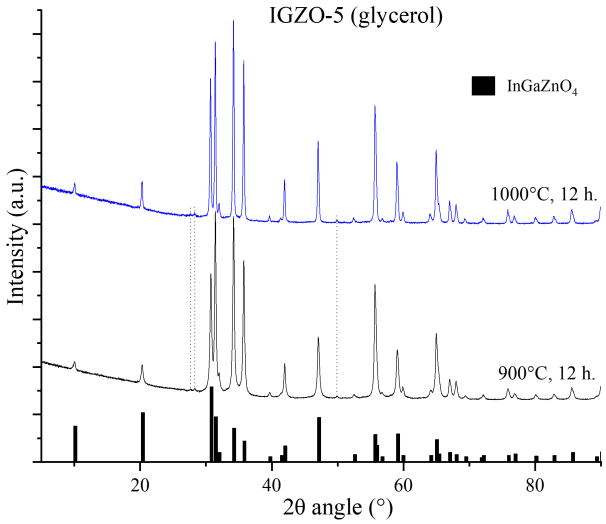

FIG. 11. XRD pattern of IGZO-5 prepared at 1000 °C. Black lines – $InGaZnO_4$ [17]

TABLE 1. Unit cell parameters of homogeneous $InGaZnO_4$ samples

No.	Sample	Unit cell parameters					
		a, Å	c, Å	a, Å	c, Å	a, Å	c, Å
Sintering temperature		700 °C		900 °C		1000 °C	
1	IGZO-1	3.300(3)	26.17(3)	3.298(2)	26.11(2)	3.295(2)	26.13(2)
2	IGZO-2	3.307(3)	26.15(3)	3.296(2)	26.11(2)	3.295(2)	26.11(2)
3	IGZO-5	3.317(5)	26.11(4)	3.297(3)	26.11(2)	3.297(2)	26.14 (2)

TABLE 2. Crystallite sizes of homogeneous $InGaZnO_4$ samples

No.	Sintering temperature		700 °C	900 °C	1000 °C
1	Crystallite size (Å)	IGZO-1	68 ± 9	221 ± 30	466 ± 59
2		IGZO-2	50 ± 8	439 ± 68	579 ± 124
3		IGZO-5	54 ± 6	242 ± 32	406 ± 56

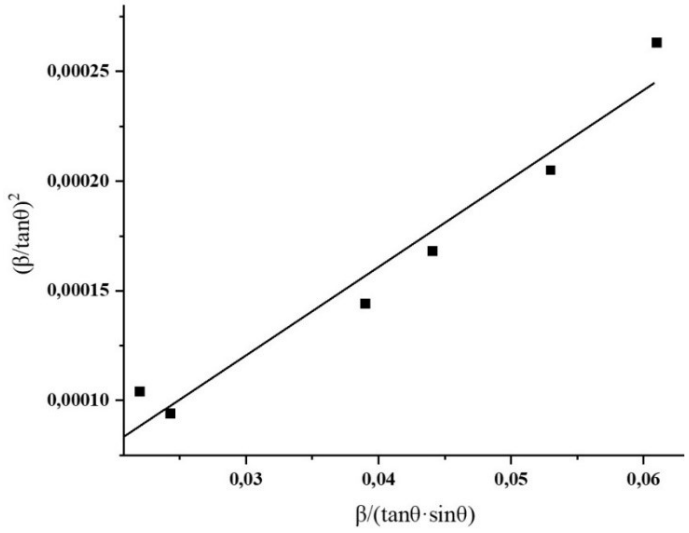

FIG. 12. Illustration for calculating crystallite size using the Halder–Wagner method for IGZO-5 obtained at 1000 °C

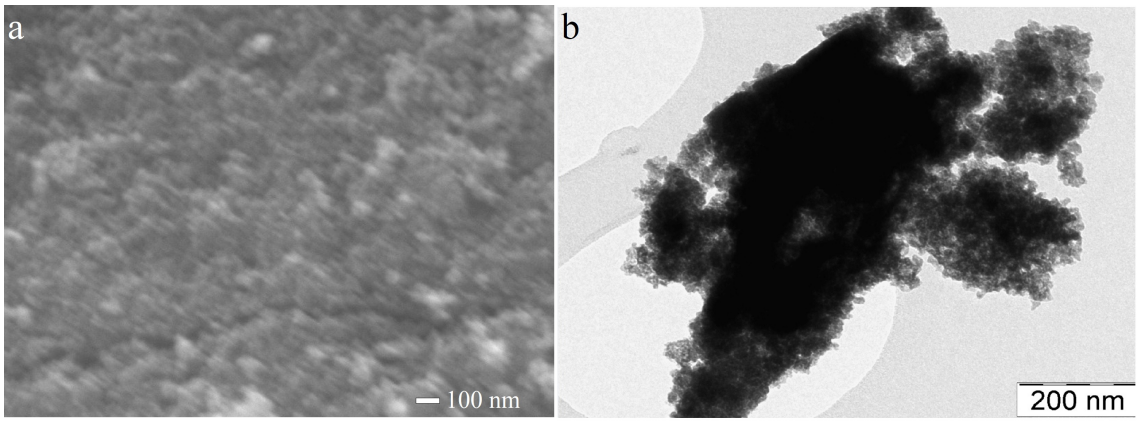

FIG. 13. SEM- (a) and TEM-image (b) of IGZO-5 prepared at 500 °C for 6 hours

20 – 30 nm, but there are areas where the particle size is much smaller. At the same time, it is worth saying that the material does not have a specific morphology. It was shown that indium gallium zinc oxide nanoparticles were obtained.

4. Conclusions

It has been shown that the use of various complexing agents in the sol-gel method affects the phase composition of the product in the In–Ga–Zn–O system. The best complexing agents for producing $InGaZnO_4$ by the sol-gel method are ethylene glycol and glycerol. The samples obtained using ethylene glycol and glycerol have an amorphous structure at 500 °C and a high degree of crystallinity at 700 – 900 °C. The use of citric acid as a complexing agent is relatively successful, but temperatures above 1000 °C are required to completely homogenize the sample. This casts doubt on the use of this complexing agent for the production of $InGaZnO_4$ ternary oxide nanoparticles. The use of urea and sucrose results in indium gallium zinc oxide contaminated with indium oxide phase. The use of oxalic acid results in the formation of a three-phase product. The samples have a crystallite size in the nano-region at temperatures of 500 – 700 °C, that was confirmed and demonstrated for IGZO-5 (500 °C, 6 h) sample by SEM and TEM method.

References

[1] Kim G.H., Kim H.S., Shin H.S., Ahn B.D., Kim K.H., Kim H.J. Inkjet-printed InGaZnO thin film transistor. *Thin Solid Films*, 2009, **517** (14), P. 4007–4010.

[2] Wang Y., Sun X.W., Goh G.K.L., Demir H.V., Yu H.Y. Influence of Channel Layer Thickness on the Electrical Performances of Inkjet-Printed In-Ga-Zn Oxide Thin-Film Transistors. *IEEE Trans. Electron Devices*, 2011, **58** (2), P. 480–485.

[3] Lee Y.G., Choi W.-S. Electrohydrodynamic Jet-Printed Zinc-Tin Oxide TFTs and Their Bias Stability. *ACS Appl. Mater. Interfaces*, 2014, **6** (14), P. 11167–11172.

[4] Jeong S., Lee J-Y., Lee S.S., Oh S-W., Lee H.H., Seo Y.-H., Ryu B.-H., Choi Y. Chemically improved high performance printed indium gallium zinc oxide thin-film transistors. *J. Mater. Chem.*, 2011, **21** (43), P. 17066–17070.

[5] Fukuda N., Watanabe Y., Uemura S., Yoshida Y., Nakamura T., Ushijima H. In-Ga-Zn oxide nanoparticles acting as an oxide semiconductor material synthesized via a coprecipitation-based method. *J. Mater. Chem. C*, 2014, **2** (13), P. 2448–2454.

[6] Pechini M.P. Method of Preparing Lead and Alkaline Earth Titanates and Niobates and Coating Method Using the Same to Form a Capacitor. US Patent 3330697, 1967.

[7] Chernukha A.S., Zvereva A.A., Zirnik G.M., Pashnin D.R., Mustafina K.E., Belyaev I.E., Dyukova O.V., Artyukova M.V., Malev E.V., Zhivulin V.E., Mosunova T.V., Vinnik D.A. Synthesis of Barium Hexaferrite by the Self-combustion Method. *Bull. South Ural State Univ. Ser. "Chemistry"*, 2021, **13** (3), P. 40–48.

[8] Kumar R., Kumar H., Singh R.R., Barman P.B. Variation in magnetic and structural properties of Co-doped Ni-Zn ferrite nanoparticles: a different aspect. *J. Sol-Gel Sci. Technol.*, 2016, **78** (3), P. 566–575.

[9] Bhagwat V.R., Humbe A.V., More S.D., Jadhav K.M. Sol-gel auto combustion synthesis and characterizations of cobalt ferrite nanoparticles: Different fuels approach. *Mater. Sci. Eng. B*, 2019, **248**, 114388.

[10] Khort A., Hedberg J., Mei N., Romanovski V., Blomberg E., Odnevall I. Corrosion and transformation of solution combustion synthesized Co, Ni and CoNi nanoparticles in synthetic freshwater with and without natural organic matter. *Sci. Rep.*, 2021, **11** (1), 7860.

[11] Oladoja N.A., Anthony E.T., Ololade I.A., Saliu T.D., Bello G.A. Self-propagation combustion method for the synthesis of solar active Nano Ferrite for Cr(VI) reduction in aqua system. *J. Photochem. Photobiol. A Chem.*, 2018, **353**, P. 229–239.

[12] Yadav R.S., Kuřitka I., Vilcakova J., Machovsky M., Skoda D., Urbánek P., Masař M., Jurča M., Urbánek M., Kalina L., Havlica J. NiFe2O4 Nanoparticles Synthesized by Dextrin from Corn-Mediated Sol-Gel Combustion Method and Its Polypropylene Nanocomposites Engineered with Reduced Graphene Oxide for the Reduction of Electromagnetic Pollution. *ACS Omega*, 2019, **4** (26), P. 22069–22081.

[13] Wahba M.A., Yakout S.M., Youssef A.M., Sharmoukh W., Elsayed A.M., Khalil M.Sh. Chelating Agents Assisted Rapid Synthesis of High Purity $BiFeO_3$: Remarkable Optical, Electrical, and Magnetic Characteristics. *J. Supercond. Nov. Magn.*, 2022, **35** (12), P. 3689–3704.

[14] Katelnikovas A., Barkauskas J., Ivanauskas F., Beganskiene A., Kareiva A. Aqueous sol-gel synthesis route for the preparation of YAG: Evaluation of sol-gel process by mathematical regression model. *J. Sol-Gel Sci. Technol.*, 2007, **41**, P. 193–201.

[15] Yu L., Sun A. Influence of different complexing agents on structural, morphological, and magnetic properties of Mg-Co ferrites synthesized by sol-gel auto-combustion method. *J. Mater. Sci. Mater. Electron.*, 2021, **32** (8), P. 10549–10563.

[16] Momma K., Izumi F. VESTA 3 for three-dimensional visualization of crystal, volumetric and morphology data. *J. Appl. Crystallogr.*, 2011, **44** (6), P. 1272–1276.

[17] Kimizuka N., Mohri T. Spinel, $YbFe_2O_4$, and $Yb_2Fe_3O_7$ types of structures for compounds in the In_2O_3 and Sc_2O_3–A_2O_3–BO systems [A: Fe, Ga, or Al; B: Mg, Mn, Fe, Ni, Cu, or Zn] at temperatures over 1000 °C. *J. Solid State Chem.*, 1985, **60** (3), P. 382–384.

[18] Nespolo M., Sato A., Osawa T., Ohashi H. Synthesis, crystal structure and charge distribution of $InGaZnO_4$. X-ray diffraction study of 20 kb single crystal and 50 kb twin by reticular merohedry. Cryst. Res. Technol. 2000, 35(2), P. 151–165.

[19] Xu C., Jiang P., Cong R., Yang T. Structure investigation of $InGaZn_{1-x}Cu_xO_4$ (x = 0–1) and magnetic property of $InGaCuO_4$. *J. Solid State Chem.*, 2019, **274**, P. 303–307.

[20] Mohamed S.H. Transparent conductive gallium-doped indium oxide nanowires for optoelectronic applications. *J. Korean Phys. Soc.*, 2013, **62** (6), P. 902–905.

[21] Yang J., Sun X., Yang W., Zhu M., Shi J. The Improvement of Coralline-Like $ZnGa_2O_4$ by Cocatalysts for the Photocatalytic Degradation of Rhodamine *B. Catalysts*, 2020, **10** (2), 221.

[22] Zhivulin V.E., Trofimov E.A., Zaitseva O.V., Sherstyuk D.P., Cherkasova N.A., Taskaev S.V., Vinnik D.A., Alekhina Y.A., Perov N.S., Naidu K.C.B., Elsaeedy H.I., Khandaker M.U., Tishkevich D.I., Zubar T.I., Trukhanov A.V., Trukhanov S.V. Preparation, phase stability, and magnetization behavior of high entropy hexaferrites. *iScience*, 2023, **26** (7), 107077.

[23] Vinnik D.A., Sherstyuk D.P., Zhivulin V.E., Zhivulin D.E., Starikov A.Yu., Gudkova S.A., Zherebtsov D.A., Pankratov D.A., Alekhina Yu.A., Perov N.S., Trukhanov S.V., Trukhanova E.L., Trukhanov A.V. Impact of the Zn–Co content on structural and magnetic characteristics of the Ni spinel ferrites. *Ceram. Int.*, 2022, **48** (13), P. 18124–18133.

[24] Nath D., Singh F., Das R. X-ray diffraction analysis by Williamson-Hall, Halder-Wagner and size-strain plot methods of CdSe nanoparticles – a comparative study. *Mater. Chem. Phys.*, 2020, **239**, 122021.

Submitted 7 June 2024; accepted 8 August 2024

Information about the authors:

Gleb M. Zirnik – Moscow Institute of Physics and Technology, Laboratory of Semiconductor Oxide Materials, Institutsky lane, 9, Dolgoprudny, 141701, Russia; St. Petersburg State University, Institute of Chemistry, Universitetskaya emb., 7–9, 199034, St. Petersburg, Russia; ORCID 0009-0008-4546-1368; glebanaz@mail.ru

Alexander S. Chernukha – Moscow Institute of Physics and Technology, Laboratory of Semiconductor Oxide Materials, Institutsky lane, 9, Dolgoprudny, 141701, Russia; St. Petersburg State University, Institute of Chemistry, Universitetskaya emb., 7–9, 199034, St. Petersburg, Russia; ORCID 0000-0002-7117-7132; chernukha.as@mipt.ru;

Daniil A. Uchaev – South Ural State University, Scientific and Educational Center "Nanotechnologies", Lenin Av., 76, Chelyabinsk, 454080, Russia; ORCID 0000-0002-8623-4769; uchaevda@susu.ac.ru

Ibrohimi A. Solizoda – Moscow Institute of Physics and Technology, Laboratory of Semiconductor Oxide Materials, Institutsky lane, 9, Dolgoprudny, 141701, Russia; St. Petersburg State University, Institute of Chemistry, Universitetskaya emb., 7–9, 199034, St. Petersburg, Russia; Tajik National University, Rudaki Av., 17, Dushanbe, 734025, Tajikistan; ORCID 0000-0001-6973-4633 ; solizoda.ia@mipt.ru

Svetlana A. Gudkova – Moscow Institute of Physics and Technology, Laboratory of Semiconductor Oxide Materials, Institutsky lane, 9, Dolgoprudny, 141701, Russia; St. Petersburg State University, Institute of Chemistry, Universitetskaya emb., 7–9, 199034, St. Petersburg, Russia, ORCID 0000-0002-3028-947X; svetlanagudkova@yandex.ru

Nadezhda S. Nekorysnova – South Ural State University, Scientific and Educational Center “Nanotechnologies”, Lenin Av., 76, Chelyabinsk, 454080, Russia; ORCID 0009-0002-1921-7915; nadin5004@mail.ru

Denis A. Vinnik – Moscow Institute of Physics and Technology, Laboratory of Semiconductor Oxide Materials, Institutsky lane, 9, Dolgoprudny, 141701, Russia; St. Petersburg State University, Institute of Chemistry, Universitetskaya emb., 7–9, 199034, St. Petersburg, Russia; South Ural State University, Scientific and Educational Center “Nanotechnologies”, Lenin Av., 76, Chelyabinsk, 454080, Russia; ORCID 0000-0002-5190-9834; vinnik.da@mipt.ru

Conflict of interest: the authors declare no conflict of interest.